RSC Advances

PAPER

View Article Online
View Journal | View Issue

Cite this: *RSC Adv.*, 2019, **9**, 21557

Design strategies for the development of a Pd-based acetylene hydrochlorination catalyst: improvement of catalyst stability by nitrogen-containing ligands†

Haihua He,[ab] Jia Zhao, *[a] Bolin Wang,[a] Yuxue Yue,[a] Gangfeng Sheng,[a] Qingtao Wang,[a] Lu Yu,[a] Zhong-Ting Hu[c] and Xiaonian Li*[a]

Acetylene hydrochlorination is an attractive chemical reaction for the manufacture of polyvinyl chloride (PVC), and the development efforts are focused on the search for non-mercury catalyst systems. Supported Pd-based catalysts have relatively high activity in the catalytic hydrochlorination of acetylene but are still deactivated rather quickly. Herein, we demonstrated that the atomically dispersed $(NH_4)_2PdCl_4$ complex, distributed on activated carbon, enabled the highly active and stable production of the vinyl chloride monomer (VCM) through acetylene hydrochlorination under low temperature conditions. We found that the presence of nitrogen-containing ligands in the structure of the active center could remarkably improve the stability of the Pd-based catalysts when compared with the case of the conventional $PdCl_2$ catalyst. Further analyses *via* X-ray diffraction (XRD), transmission electron microscopy (TEM), X-ray photoelectron spectroscopy (XPS) and temperature-programmed reduction (TPR) show that the variations in the Pd dispersion, chemical state and reduction property are caused by the nitrogen-containing ligands. Temperature-programmed desorption (TPD) characterizations illustrated that the N-containing ligands over the $(NH_4)_2PdCl_4$/AC catalyst might enhance the adsorption of HCl. These findings suggest that in addition to strategies that target the doping modification of support materials, optimization of the structure of the active center complexes provides a new path for the design of highly active and stable Pd-based catalysts.

Received 5th April 2019
Accepted 26th June 2019

DOI: 10.1039/c9ra02572c

rsc.li/rsc-advances

1 Introduction

Polyvinyl chloride (PVC) is commonly used in various manufacturing processes due to its advanced performance in mechanical enhancement, chemical inertness and stability. PVC is produced by the polymerization of the vinyl chloride monomer (VCM), synthesized either *via* the oxychlorination reaction of ethylene or *via* hydrochlorination of acetylene, and the latter approach usually employs supported mercuric chloride as a catalyst.[1–3] However, mercuric chloride vapor may release into the environment easily under the reaction conditions and poison human beings and the environment.[4,5] The Minamata Convention on Mercury was approved by delegates from over 140 countries in 2013 for limiting the emission and use of hazardous mercury, and now, the treaty has entered into force. Considering the current severe mercury limitations, it is urgent to develop a new mercury-free catalyst for this process.

As the selection of non-mercury catalysts poses a significant challenge, a number of catalytic formulations have been proposed including noble metal chlorides,[6–29] non-noble metal chlorides[30–35] and even non-metallic materials.[36–44] Among them, Pd catalysts have been considered to be very effective for the hydrochlorination of acetylene. For example, Hutchings *et al.* explored the catalytic performance of carbon supported with a series of metal chlorides and found that the conversion of acetylene to VCM decreased in the following order: Pd(II) > Hg(II) > Cu(II) ~ Cu(I) > Ag(I) > Cd(II) > Zn(II).[45] Although the Pd-based catalysts exhibited excellent hydrochlorination activity, similar to most other precious metal catalysts, they could not maintain a high level of stability. It appears that the inherent volatilization loss of the Pd active species restrains the application of Pd-based catalysts for the hydrochlorination of acetylene. Therefore, the stabilization of volatile Pd active species under the reaction conditions has become an urgent technical issue to make acetylene hydrochlorination applicable.

To date, the main strategies used for the stabilization of Pd species are still focused on the doping modification of support materials to improve the stability of the metal catalysts by

[a]*Industrial Catalysis Institute, Laboratory Breeding Base of Green Chemistry-Synthesis Technology, Zhejiang University of Technology, Hangzhou 310014, China. E-mail: jiazhao@zjut.edu.cn; xnli@zjut.edu.cn; Tel: +86 571 88320002*

[b]*Pharmaceutical and Material Engineering School, Jin Hua Polytechnic, Jinhua 321007, China*

[c]*College of Environment, Zhejiang University of Technology, Hangzhou 310014, China*

† Electronic supplementary information (ESI) available. See DOI: 10.1039/c9ra02572c

enhancing the interactions of the Pd species with the supports. For example, Wang *et al.* showed that upon adjusting the surface acidity of the support, an NH_4F-modified Pd/HY catalyst delivered enhanced stability;[46] Bao *et al.* showed that upon doping of the carbon structure with certain nitrogen species, the stability of the $PdCl_2$/AC-N catalyst was significantly improved.[47] These experimental results suggest that one of the effective solutions to overcome the volatilization issue of Pd species is to develop a suitable support that can exhibit enhanced interaction with the Pd active centers. However, only few studies have been reported on the optimization of the structure of the active center to enhance the catalytic performance of Pd-based catalysts. Recently, it has been found that the coordination of an ionic liquid to the Pd active center can stabilize the Pd species against volatilization and then improve the catalytic stability.[48] In this study, the well-defined $(NH_4)_2PdCl_4$ complex was prepared, and an attempt was made to explore the catalytic performance of the carbon-supported $(NH_4)_2PdCl_4$ complex catalysts. It was found that the $(NH_4)_2PdCl_4$ active center could significantly stabilize the Pd species. Furthermore, the stabilization mechanism of Pd species in the $(NH_4)_2PdCl_4$/AC catalyst was proposed on the basis of TEM, XPS, ICP, H_2-TPR and TPD characterization. To the best of our knowledge, this is the first study that reports the use of nitrogen-containing Pd complexes in the preparation of supported Pd-based catalysts for acetylene hydrochlorination.

2 Experimental

2.1 Catalyst preparation

The $(NH_4)_2PdCl_4$ complex was synthesized according to the literature.[49,50] The representative procedures were conducted as follow: 35.3 mg H_2PdCl_4 (Sigma-Aldrich) and 23 mg NH_4Cl (Sigma-Aldrich) were dissolved in 8 ml water at 80 °C *via* ultrasonication for 60 min to obtain yellow-brown $(NH_4)_2PdCl_4$ crystals, and then, the catalyst preparation was conducted using an incipient wetness impregnation technique; after this, 3 g of active carbon was added to the abovementioned mixture under agitation. After drying the mixture for 12 h at 110 °C in an oven under vacuum, the synthesized catalyst was obtained, named $(NH_4)_2PdCl_4$/AC. A carbon-supported $PdCl_2$ catalyst ($PdCl_2$/AC) was synthesized as a reference catalyst following the abovementioned methods except for the addition of the reagent NH_4Cl. Unless otherwise specified, the loading amount of Pd in all Pd-based catalysts was 0.5 wt%.

2.2 Catalyst characterization

XPS spectra were obtained by the Kratos AXIS Ultra DLD apparatus, with a monochromatized aluminum X-ray source, and the passing energy was 40 eV. The C 1s line (284.8 eV) was adopted as the corrected benchmark for all the measured spectra. The specific surface areas were measured using N_2 adsorption–desorption at 77 K *via* the Micromeritics ASAP 2000 instrument. TEM was used to characterize the catalyst morphology and microstructures *via* the Tecnai G2 F30 S-Twin electron microscope. The TPD was conducted in a tubular quartz reactor. Herein, 75 mg of each catalyst sample was initially treated with pure C_2H_2 or HCl at 180 °C for 30 min; after adsorption and sweeping with pure Ar for 60 min at the gas flow rate of 30 ml min^{-1}, a temperature-programmed route was carried out from 25 °C to 550 °C at the heating rate of 10 °C min^{-1}.

2.3 Catalytic test

Activity tests for the hydrochlorination of acetylene were conducted in a heterogeneous fixed-bed reactor. Prior to the reaction, nitrogen (N_2) was passed through the reactor for 30 min to remove any water and air remaining. Then, C_2H_2 (5 ml min^{-1}, 1 bar) and HCl (6 ml min^{-1}, 1 bar) were added to the clean and dry reactor using a mass flow controller. The output gas products were passed through a vessel with the NaOH solution to remove excess HCl. The composition of the output was analyzed by gas chromatography (GC-9790A).

3 Results and discussion

3.1 Catalytic performance of Pd-based catalysts

The catalytic performances of $(NH_4)_2PdCl_4$/AC and $PdCl_2$/AC catalysts are shown in Fig. 1 at the reaction temperature of 100 °C and C_2H_2 GHSV of 100 h^{-1}. We could observe that the $(NH_4)_2PdCl_4$/AC catalyst showed superior catalytic performance than that of the $PdCl_2$/AC catalyst, resulting in a 99.7% acetylene conversion (Fig. 1a) and 99.5% VCM selectivity (Fig. 1b). Compared with $PdCl_2$/AC, the $(NH_4)_2PdCl_4$/AC catalyst also shows a remarkable robust catalytic behavior under these conditions. Note that the acetylene activity of the catalyst $(NH_4)_2PdCl_4$ at this low temperature (100 °C) was equivalent to that of the typical Pd-based catalyst reported at high temperatures (typically exceeding 140 °C, as listed in Table S1†).

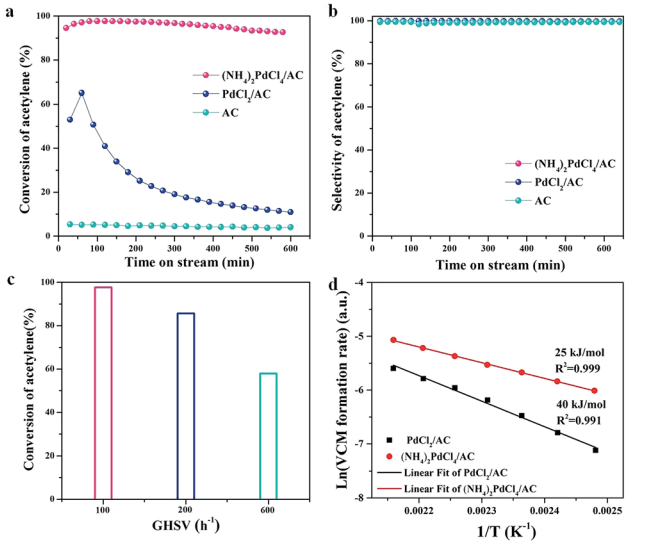

Fig. 1 (a) Conversion of C_2H_2 and (b) selectivity to VCM over $(NH_4)_2PdCl_4$/AC, $PdCl_2$/AC and AC catalysts. Reaction conditions: T = 100 °C, GHSV(C_2H_2) = 100 h^{-1}, and HCl/C_2H_2 = 1.2. (c) Catalytic activity of $(NH_4)_2PdCl_4$/AC as a function of space velocities. Reaction conditions: T = 100 °C and HCl/C_2H_2 = 1.2. (d) Arrhenius plot for VCM formation using the $(NH_4)_2PdCl_4$/AC and $PdCl_2$/AC catalysts.

The effect of space velocity on the hydrochlorination of acetylene was further investigated. As shown in Fig. 1c, the acetylene conversion remained at 85% and 57% as the space velocity of C_2H_2 was increased from 100 h^{-1} to 200 h^{-1} and then to 600 h^{-1} at 100 °C, respectively. We have demonstrated that the designed $(NH_4)_2PdCl_4$/AC catalyst is suitable for the hydrochlorination of acetylene in a wide range of space velocities.

To further clarify the structural evolution of the active phase for $PdCl_2$/AC and $(NH_4)_2PdCl_4$/AC, the kinetic behaviors were discussed by calculating the approximate activation energy (E_a) (Fig. 1d). Ea was calculated based on the Arrhenius plots (ln(R) *versus* 1/T), and all the kinetic data were obtained and calculated at the level of <15% yield of vinyl chloride, which excluded the effect of internal and external diffusion. Contrary to the E_a calculated for the $PdCl_2$/AC catalyst, the E_a of $(NH_4)_2PdCl_4$/AC was markedly decreased from 40 to 25 kJ mol^{-1}. The improvement in the catalytic performance may be assigned to the modulation of the intrinsic structure of the catalysts as well as the synergetic effect of Pd and the nitrogen-containing ligands on the catalytic performance.

3.2 Catalytic characterization

As shown, $(NH_4)_2PdCl_4$/AC illustrated excellent catalytic performance for the hydrochlorination of acetylene. To elucidate the influence of nitrogen-containing ligands on the catalyst microstructure, valence and adsorption properties, a series of structural characterizations were employed to analyze the Pd-based catalysts. XRD analysis was employed to probe the characteristics of the support and the Pd species. No discernible Pd^0 characteristic diffraction peaks were observed in the XRD patterns of the fresh $(NH_4)_2PdCl_4$/AC and $PdCl_2$/AC catalysts; this suggested that most of the Pd species were present in small nanoclusters and/or non-crystalline isolated atoms (Fig. 2).

Fig. 3 shows an HAADF-STEM image of the $(NH_4)_2PdCl_4$/AC and $PdCl_2$/AC catalysts. As observed, the HAADF-STEM analysis clearly demonstrated the existence of isolated Pd atoms with high number density in $(NH_4)_2PdCl_4$/AC (Fig. 3a). They are observed as bright spots evenly distributed on the surface of carbon. The light dots cannot be attributed to nitrogen species as nitrogen species cannot be distinguished from carbon in the current analysis mode. Therefore, the light dots must be assigned to Pd species. Furthermore, since the light gray dot has the typical size of 2–3 Å, these dots should be mainly assigned to single atoms/cations. For $PdCl_2$/AC, it can be observed that except for the presence of isolated Pd atoms as big bright white spots, the image also illustrates the presence of Pd clusters with a few atoms (Fig. 3b). This observation provides a good reason to believe that the single isolated Pd atoms can be the active sites for the reaction, providing the observed promotion of the catalytic activity. More importantly, except for the amorphous diffraction peaks of carbon, no discernible diffraction peak was detected in the XRD pattern of the used $(NH_4)_2PdCl_4$/AC and $PdCl_2$/AC catalysts (Fig. 2); this indicated that the used Pd-based catalysts did not show the aggregation of particles.

Further insights into the material structure were obtained by X-ray photoelectron spectroscopy, and the deconvolution

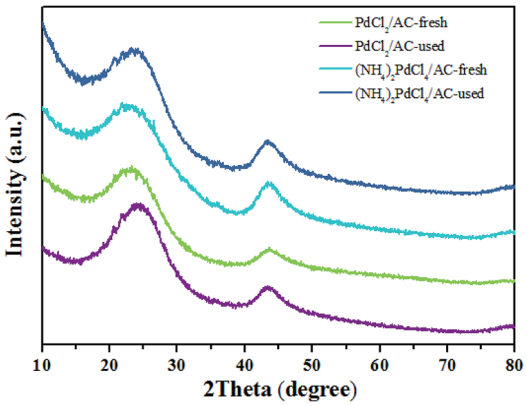

Fig. 2 XRD patterns of the $(NH_4)_2PdCl_4$/AC and $PdCl_2$/AC catalysts.

results are shown in Table 1 and Fig. 4. It is apparent that the catalyst prepared with the $(NH_4)_2PdCl_4$ precursor presents a relatively high amount of N species (3.12%), which is absent in the $PdCl_2$/AC sample; this indicates that nitrogen-containing ligands can remain stable during the preparation process. More importantly, the proportion of surface N/C has no dramatic changes before and after the reaction (Table 1 and Fig. 4b); this indicates that the $(NH_4)_2PdCl_4$ phase does not obviously decompose during the reaction. The structure of the $(NH_4)_2PdCl_4$ phase can remain relatively stable on the AC support. In addition, the surface content of Pd is 0.32% and 0.31% for the fresh $(NH_4)_2PdCl_4$/AC and $PdCl_2$/AC catalysts according to the XPS analysis, respectively, suggesting that the Pd species have been well dispersed on the support. After the reaction, the content of the Pd species reduces obviously to only 0.18% for $PdCl_2$/AC; this may be explained by the leaching of Pd

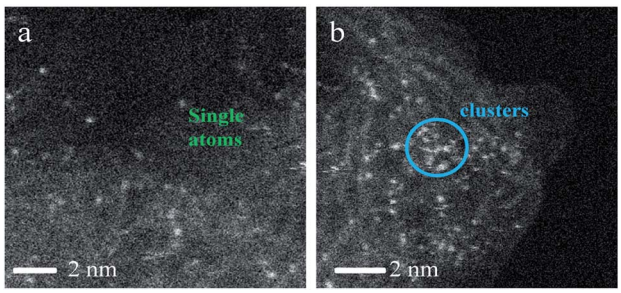

Fig. 3 Aberration-corrected HAADF-STEM images of the (a) $(NH_4)_2PdCl_4$/AC and (b) $PdCl_2$/AC catalysts.

Table 1 Surface composition of the fresh and used $(NH_4)_2PdCl_4$/AC and $PdCl_2$/AC catalyst, determined by XPS

	Elemental composition (wt%)			
Catalysts	C	Cl	Pd	N
Fresh $(NH_4)_2PdCl_4$/AC	94.28	2.28	0.32	3.12
Fresh $PdCl_2$/AC	97.12	2.57	0.31	—
Used $(NH_4)_2PdCl_4$/AC	93.62	3.14	0.28	2.96
Used $PdCl_2$/AC	95.26	4.56	0.18	—

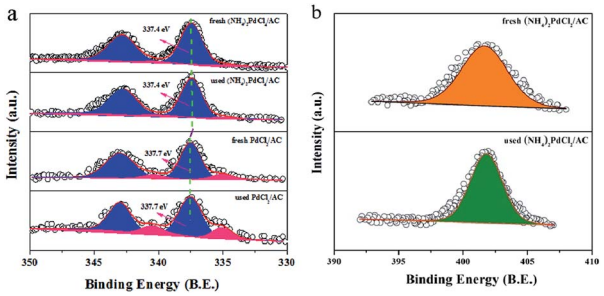

Fig. 4 (a) XPS spectra and simulation of the fresh and used $(NH_4)_2PdCl_4$/AC and $PdCl_2$/AC catalysts. (b) N 1s spectra for the fresh and used $(NH_4)_2PdCl_4$/AC catalyst.

species; by contrast, there is a negligible change in the content of the Pd species for the used $(NH_4)_2PdCl_4$/AC catalyst, which may be fairly stable in the reaction environment. Consistent with the XPS analysis, the ICP results of the fresh and used $(NH_4)_2PdCl_4$/AC and $PdCl_2$/AC catalysts also revealed that the Pd species was more stable in the presence of nitrogen-containing ligands (Table 2). Actually, the leaching of the $PdCl_2$ active component was often thought to be the cause of deactivation for Pd-based catalysts in the hydrochlorination of acetylene.[44–46,51,52] For example, Wang[41] demonstrated that 44.7% Pd species had leached from HY zeolite-supported Pd-based catalysts after reaction; in addition, Wang suggested that the Pd loss was responsible for the deactivation of the Pd/HY catalysts, and the ICP analysis indicated that about 37.8% Pd species had been lost after 10 h time on stream as compared to the case of the fresh catalyst.

Fig. 4a displays the high-resolution spectra for the Pd 3d regions of Pd-based catalysts. The binding energies of the Pd $3d_{5/2}$ signals for the fresh $(NH_4)_2PdCl_4$/AC catalyst at 337.4 eV and 335.1 eV correspond to the Pd^{2+} and Pd^0 species (Fig. 4a).[53,54] It is well-accepted that Pd in the cationic form works as an active species for acetylene hydrochlorination. However, the Pd $3d_{5/2}$ signals of the $(NH_4)_2PdCl_4$/AC catalyst, corresponding to Pd^{2+}, which represent a negative shift of 0.3 eV as compared to that of the $PdCl_2$/AC catalyst (337.7 eV), demonstrate that the electronic structure of Pd changes with the incorporation of nitrogen-containing ligands. Table 3 lists the relative ratio of Pd^{2+}/Pd^0 for the fresh and used Pd-based catalysts. The results indicate that the Pd^{2+}/Pd^0 ratio in the used catalysts observably decreases when compared with that for the fresh catalysts; this indicates that the active Pd^{2+} species has been reduced under the reaction conditions. However, the $(NH_4)_2PdCl_4$/AC catalyst experiences a slower reduction during the reaction for the Pd^{2+} species when compared with the $PdCl_2$/AC catalyst. This is likely one of the reasons for the rapid deactivation observed for $PdCl_2$/AC as compared to that of $(NH_4)_2PdCl_4$/AC. Thus, nitrogen-containing ligand modalities that can enhance the stability of the Pd^{2+} species are very important for the practical applications of these catalysts.

Table 2 Pd contents of the fresh and used $(NH_4)_2PdCl_4$/AC and $PdCl_2$/AC catalysts, determined by ICP

Catalysts	Nominal loading wt%	Results of ICP (wt%)		Loss ratio of Pd (%)
		Fresh	Used	
$(NH_4)_2PdCl_4$/AC	0.5	0.52	0.46	11.5
$PdCl_2$/AC	0.5	0.53	0.32	39.6

Table 3 The relative ratio of Pd^{2+}/Pd^0 for Pd-based catalysts

Catalysts	Pd^{2+}/Pd^0 ratio
Fresh $(NH_4)_2PdCl_4$/AC	14.46
Used $(NH_4)_2PdCl_4$/AC	14.07
Fresh $PdCl_2$/AC	7.54
Used $PdCl_2$/AC	6.34

H_2-TPR was employed to analyse the reduction ability of the active cationic Pd species. For both $PdCl_2$/AC and $(NH_4)_2PdCl_4$/AC, a discernible characteristic reduction band in the range of 500–800 °C can be observed (Fig. 5). This band was attributed to the reduction of the surface oxygenated groups on the AC support.[55] Apart from this, the clear bands at around 160–250 °C were due to the reduction of the cationic Pd species. The TPR profiles were analyzed by peak-differentiation-imitating analysis (Fig. S1†).[56] Through calibration with a CuO standard, the Pd^{2+} content for the fresh catalysts can be estimated (Table S2†); the estimated Pd^{2+} contents for the fresh $PdCl_2$/AC and $(NH_4)_2PdCl_4$/AC catalysts are *ca.* 76.3% and 80.2%, respectively, which are consistent with the XPS analysis results. A more pronounced change occurred in the reduction temperature of the Pd^{2+} species. It can be seen clearly from the graph that for the $(NH_4)_2PdCl_4$/AC catalyst, the peak for Pd^{2+} reduction is evidently increased as compared to that of $PdCl_2$/AC (Fig. 5). The increased reduction temperature of $(NH_4)_2PdCl_4$/AC can be attributed to the existence of nitrogen-containing ligands, which probably inhibit the reduction of the cationic Pd species.

The surface areas of the Pd-based catalysts were evaluated *via* the low-temperature N_2 adsorption/desorption experiments. Table 4 lists the catalyst texture parameters of the Pd-based catalysts. It is shown that the AC support has a microporous

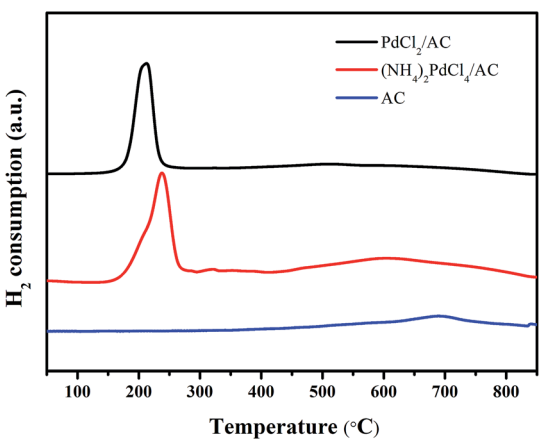

Fig. 5 H_2-TPR profiles of the fresh $(NH_4)_2PdCl_4$/AC and $PdCl_2$/AC catalysts.

Table 4 Surface areas of the AC support and Pd-based catalysts

	S_{BET} (m^2 g^{-1})		
Catalysts	Fresh	Used	ΔS_{BET} (m^2 g^{-1})
AC	1162.1	—	—
$(NH_4)_2PdCl_4$/AC	1056.1	836.5	219.6
$PdCl_2$/AC	1081.3	614.4	466.9

structure, and the specific surface area is up to 1162.1 m^2 g^{-1}. Fresh catalysts, including $PdCl_2$/AC and $(NH_4)_2PdCl_4$/AC, show specific surface areas lower than that of the AC support probably due to the blockage of pores by the active Pd species. In addition, the used catalysts exhibit lower specific surface areas when compared with those of the fresh catalysts. For example, about 43.1% of the specific surface area is lost after reaction for 10 h. The loss of the active surface area may be caused by carbon deposition (acetylene may oligomerize over the catalyst) on the catalyst surface, which may result in clogged pores and decreased catalyst activity; moreover, this is likely the cause for catalyst deactivation. However, the surface area loss was only 20.8% for $(NH_4)_2PdCl_4$/AC. This result indicates that the amount of coke deposition is significantly reduced when $(NH_4)_2PdCl_4$ is used for Pd-based catalysts although the underlying mechanism for this reduction requires further investigation.

3.3 Mechanism insight

The adsorption and activation of substrates are important steps in a catalytic reaction. Through TPD characterization, we studied the adsorption properties of the two substrates C_2H_2 and HCl over the $(NH_4)_2PdCl_4$/AC and $PdCl_2$/AC catalysts. In Fig. 6, the individual C_2H_2-TPD results exhibit that the desorption temperature of the surveyed catalysts follows the order of $PdCl_2$/AC (387 °C) < $(NH_4)_2PdCl_4$/AC (410 °C), demonstrating that $(NH_4)_2PdCl_4$/AC displays strong adsorption capacity for C_2H_2, followed by $PdCl_2$/AC. The reactivity of Pd^{2+} towards C_2H_2 is usually explained by π-coordination and σ-coordination between the Pd^{2+} and triple bond of C_2H_2; thereby, C_2H_2 is activated. In addition, by comparing the desorption temperature of C_2H_2 for the two catalysts, it was found that the adsorption capacity of $(NH_4)_2PdCl_4$/AC to C_2H_2 was stronger than that of $PdCl_2$/AC. Similar phenomena were found in the results of HCl-TPD, where $(NH_4)_2PdCl_4$/AC exhibited a stronger ability to absorb HCl than $PdCl_2$/AC. The desorption temperatures of HCl for $(NH_4)_2PdCl_4$/AC and $PdCl_2$/AC were 369 and 264 °C, respectively. From the C_2H_2- and HCl-TPD results, we can observe that the desorption content of C_2H_2 changes negatively for $(NH_4)_2PdCl_4$/AC and $PdCl_2$/AC, whereas higher HCl desorption content has been found for $(NH_4)_2PdCl_4$/AC than that for $PdCl_2$/AC. Upon comparing the coordination structures of the Pd active sites in the catalysts $(NH_4)_2PdCl_4$/AC and $PdCl_2$/AC, it was found that the difference in the HCl desorption properties might be influenced by the presence of $[NH_4]^+$ in the $(NH_4)_2PdCl_4$/AC catalysts. The existence of the basic ion $[NH_4]^+$ in the $(NH_4)_2PdCl_4$ catalyst promoted the adsorption of acidic HCl molecules. In addition, because the differences between the HCl desorption temperatures and desorption contents of $(NH_4)_2PdCl_4$/AC and $PdCl_2$/AC are significantly high, HCl may be adsorbed on different sites: HCl is likely adsorbed on Pd^{2+} of the $PdCl_2$/AC catalyst and $[NH_4]^+$ of the $(NH_4)_2PdCl_4$/AC catalyst. Moreover, previous studies have shown that once the Pd-based catalyst is exposed to the feed gases, only C_2H_2 can be adsorbed on Pd^{2+} and HCl cannot be adsorbed due to the stronger adsorptive capacity of the catalyst for C_2H_2 than that for HCl. Under these conditions, the reaction follows the typical E–R mechanism for the classical $PdCl_2$/AC catalyst; that is, HCl reacts with the adsorbed C_2H_2 on Pd^{2+} to produce vinyl chloride.

Since HCl can be adsorbed by $[NH_4]^+$, which indicates that the HCl molecule is activated during the adsorption process, there is another possibility for the mechanism of acetylene hydrochlorination over the $(NH_4)_2PdCl_4$/AC catalyst. The possible reaction mechanism is shown in Fig. 6c. The proposed reaction mechanism was further validated by kinetic experiments. As mentioned in Fig. 1d, compared with the E_a calculated from $PdCl_2$/AC, the E_a of the $(NH_4)_2PdCl_4$/AC catalyst decreases significantly from 40 to 25 kJ mol^{-1}. This is precisely due to the further activation of HCl molecules on $[NH_4]^+$ such that the energy required for the reaction becomes lower. Under the same conditions, $(NH_4)_2PdCl_4$/AC exhibits a higher catalytic performance than $PdCl_2$/AC, as shown in Fig. 1a.

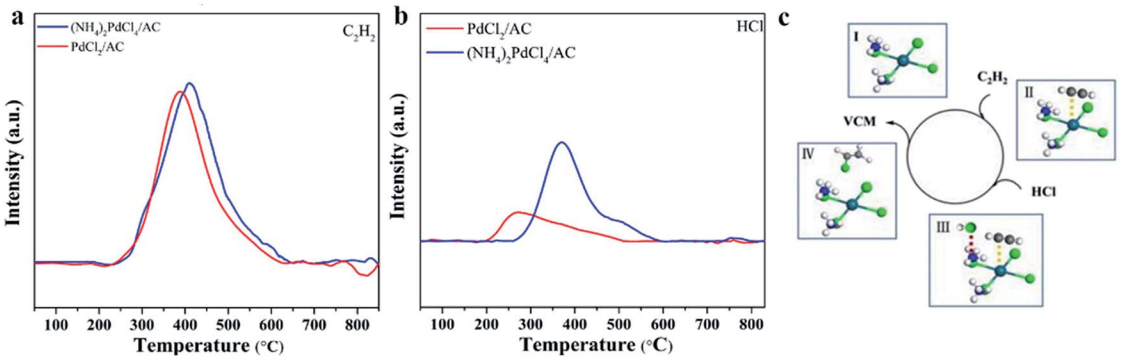

Fig. 6 (a) C_2H_2-TPD and (b) HCl-TPD profiles of the fresh $(NH_4)_2PdCl_4$/AC and $PdCl_2$/AC catalysts; and (c) the proposed catalytic mechanism for the $(NH_4)_2PdCl_4$/AC catalyst.

4 Conclusions

In summary, we adopted an innovative strategy to synthesize non-mercury catalysts using the compound $(NH_4)_2PdCl_4$ instead of traditional $PdCl_2$. The prepared catalyst $(NH_4)_2PdCl_4$/AC demonstrated excellent activity and stability in the hydrochlorination of acetylene. This indicated that the microelectronic environment of the active Pd^{2+} sites was regulated and the reduction resistance of cationic palladium was improved *via* the addition of nitrogen-containing ligands $[NH_4]^+$ to the structure of the active center. In particular, nitrogen-containing ligand additive not only can enhance the dispersion of Pd species, but can also promote the activation ability of HCl and then reduce the activation energy of the reaction. Therefore, our study proves that the $(NH_4)_2PdCl_4$/AC catalyst can be a hopeful candidate for efficient, well-stabilized non-mercury catalysts in the manufacture of vinyl chloride.

Conflicts of interest

There are no conflicts to declare.

Acknowledgements

We gratefully acknowledge the financial support provided by the National Natural Science Foundation of China (No. 21606199, 21476207), the China Postdoctoral Science Foundation (No. 2016M592015) and the Zhejiang Province Public Welfare Project (Project No. 2017C31116).

Notes and references

1 H. Schobert, *Chem. Rev.*, 2014, **114**, 1743–1760.
2 R. Lin, A. P. Amrute and J. Pérez-Ramírez, *Chem. Rev.*, 2017, **117**, 4182–4247.
3 C. J. Davies, P. J. Miedziak, G. L. Brett and G. J. Hutchings, *Chin. J. Catal.*, 2016, **37**, 1600–1607.
4 D. T. Grady and G. J. Hutchings, *Appl. Catal.*, 1985, **17**, 155–160.
5 J. Zhong, Y. Xu and Z. Liu, *Green Chem.*, 2018, **20**, 2412–2427.
6 G. J. Hutchings, *J. Catal.*, 1985, **96**, 292–295.
7 B. Nkosi, N. J. Coville and G. J. Hutchings, *J. Chem. Soc., Chem. Commun.*, 1988, **1**, 71–72.
8 M. Conte, A. F. Carley, C. Heirene, D. J. Willock, P. Johnston, A. A. Herzing, C. J. Kiely and G. J. Hutchings, *J. Catal.*, 2007, **250**, 231–239.
9 M. Conte, C. J. Davies, D. J. Morgan, A. F. Carley, P. Johnston and G. J. Hutchings, *Catal. Lett.*, 2014, **144**, 1–8.
10 P. Johnston, N. Carthey and G. J. Hutchings, *J. Am. Chem. Soc.*, 2015, **137**, 14548–14557.
11 G. Malta, S. A. Kondrat, S. J. Freakley, C. J. Davies, L. Lu, S. Dawson, A. Thetford, E. K. Gibson, D. J. Morgan, W. Jones, P. P. Wells, P. Johnston, C. R. A. Catlow, C. J. Kiely and G. J. Hutchings, *Science*, 2017, **355**, 1399–1403.
12 G. Malta, S. A. Kondrat, S. J. Freakley, C. J. Davies, S. Dawson, X. Liu, L. Lu, K. Dymkowski, F. Fernandez-Alonso, S. Mukhopadhyay, E. K. Gibson, P. P. Wells, S. F. Parker, C. J. Kiely and G. J. Hutchings, *ACS Catal.*, 2018, **8**, 8493–8505.
13 H. Y. Zhang, B. Dai, X. G. Wang, L. L. Xu and M. Y. Zhu, *J. Ind. Eng. Chem.*, 2012, **18**, 49–54.
14 S. J. Wang, B. X. Shen and Q. L. Song, *Catal. Lett.*, 2010, **134**, 102–109.
15 J. Liu, G. Lan, Y. Qiu, X. Wang and Y. Li, *Chin. J. Catal.*, 2018, **39**, 1664–1671.
16 J. Zhao, J. T. Xu, J. H. Xu, J. Ni, T. T. Zhang, X. L. Xu and X. N. Li, *ChemPlusChem*, 2015, **80**, 196–201.
17 J. Zhao, J. T. Xu, J. H. Xu, T. T. Zhang, X. X. Di, J. Ni and X. N. Li, *Chem. Eng. J.*, 2015, **262**, 1152–1160.
18 J. Zhao, T. T. Zhang, X. X. Di, J. H. Xu, S. C. Gu, Q. F. Zhang, J. Ni and X. N. Li, *Catal. Sci. Technol.*, 2015, **5**, 4973–4984.
19 B. L. Wang, J. Zhao, Y. X. Yue, G. F. Sheng, H. X. Lai, J. Y. Rui, H. H. He, Z. T. Hu, F. Feng, Q. F. Zhang, L. L. Guo and X. N. Li, *ChemCatChem*, 2019, **11**, 1002–1009.
20 J. Zhao, B. L. Wang, Y. X. Yue, S. X. Di, Y. Y. Zhai, H. H. He, G. F. Sheng, H. X. Lai, Y. H. Zhu, L. L. Guo and X. N. Li, *J. Catal.*, 2018, **365**, 153–162.
21 J. Zhao, Y. Yu, X. L Xu, S. X. Di, B. L. Wang, H. Xu, J. Ni, L. L. Guo, Z. Y. Pan and X. N. Li, *Appl. Catal., B*, 2017, **206**, 175–183.
22 J. Zhao, S. C. Gu, X. L. Xu, T. T. Zhang, Y. Yu, X. X. Di, J. Ni, Z. Y. Pan and X. N. Li, *Catal. Sci. Technol.*, 2016, **6**, 3263–3270.
23 J. Zhao, S. C. Gu, X. L. Xu, T. T. Zhang, X. X. Di, Z. Y. Pan and X. N. Li, *RSC Adv.*, 2015, **5**, 101427–101436.
24 J. Zhao, T. T. Zhang, X. X. Di, J. T. Xu, J. H. Xu, F. Feng, J. Ni and X. N. Li, *RSC Adv.*, 2015, **5**, 6925–6931.
25 S. L. Chao, Q. X. Guan and W. Li, *J. Catal.*, 2015, **330**, 273–279.
26 H. Li, B. Wu, F. Wang and X. Zhang, *ChemCatChem*, 2018, **10**, 4090–4099.
27 J. Zhao, B. L. Wang, X. L. Xu, Y. Yu, S. X. Di, H. Xu, Y. Y. Zhai, H. H. He, L. L. Guo, Z. Y. Pan and X. N. Li, *J. Catal.*, 2017, **350**, 149–158.
28 L. Ye, X. Duan, S. Wu, T. S. Wu, Y. Zhao, A. W. Robertson, H. L. Chou, J. Zheng, T. Ayvali, S. Day, C. Tang, Y. L. Soo, Y. Yuan and S. C. E. Tsang, *Nat. Commun.*, 2019, **10**, 914–923.
29 H. X. Lai, B. L. Wang, Y. Y. Yue, G. F. Sheng, S. S. Wang, F. Feng, Q. F. Zhang, J. Zhao and X. N. Li, *ChemCatChem*, 2019, DOI: 10.1002/cctc.201900710.
30 K. Zhou, J. K. Si, J. C. Jia, J. Q. Huang, J. Zhou, G. H. Luo and F. Wei, *RSC Adv.*, 2014, **4**, 7766–7769.
31 Y. F. Pu, J. L. Zhang, L. Yu, Y. H. Jin and W. Li, *Appl. Catal., A*, 2014, **488**, 28–36.
32 X. M. Wang, M. Y. Zhu and B. Dai, *ACS Sustainable Chem. Eng.*, 2019, **7**, 6170–6177.
33 Z. J. Song, G. Y. Liu, D. W. He, X. D. Pang, Y. S. Tong, Y. Q. Wu, D. H Yuan, Z. M Liu and Y. P Xu, *Green Chem.*, 2016, **18**, 5994–5998.
34 Y. Y. Zhai, J. Zhao, X. X. Di, S. X Di, B. L. Wang, Y. X. Yue, G. F. Sheng, H. X. Lai, L. L. Guo, H. Wang and X. N. Li, *Catal. Sci. Technol.*, 2018, **8**, 38159–38163.
35 J. T. Xu, J. Zhao, T. T. Zhang, X. X. Di, S. C. Gu, J. Ni and X. N. Li, *RSC Adv.*, 2015, **5**, 2901–2908.

36 X. Y. Li, X. L. Pan, L. Yu, P. J. Ren, X. Wu, L. T. Sun, F. Jiao and X. H. Bao, *Nat. Commun.*, 2014, **5**, 3688–3694.
37 K. Zhou, B. Li, Q. Zhang, J. Q. Huang, G. L. Tian, J. C. Jia, M. Q. Zhao, G. H. Luo, D. S. Su and F. Wei, *ChemSusChem*, 2014, **7**, 723–728.
38 B. L. Wang, H. X. Lai, Y. X. Yue, G. F. Sheng, Y. Q. Deng, H. H. He, L. L. Guo, J. Zhao and X. N. Li, *Catalysts*, 2018, **8**, 351–363.
39 R. Lin, S. K. Kaiser, R. Hauert and J. Pérez-Ramírez, *ACS Catal.*, 2018, **8**, 1114–1121.
40 X. Y. Li, J. L. Zhang, Y. Han, M. Y. Zhu, S. S. Shang and W. Li, *J. Mater. Sci.*, 2018, **53**, 4913–4926.
41 G. Lan, Y. Yang, X. Wang, W. Han, H. Tang, H. Liu and Y. Li, *Microporous Mesoporous Mater.*, 2018, **264**, 248–253.
42 P. Li, H. Li, X. Pan, K. Tie, T. Cui, M. Ding and X. Bao, *ACS Catal.*, 2017, **7**, 8572–8577.
43 B. L. Wang, H. X. Lai, Y. X. Yue, G. F. Sheng, Y. Q. Deng, H. H. He, L. L. Guo, J. Zhao and X. N. Li, *Catalysts*, 2018, **8**, 351–364.
44 J. Zhao, B. L. Wang, Y. X. Yue, G. F. Sheng, H. X. Lai, S. S. Wang, L. Yu, Q. F. Zhang, F. Feng, Z. T. Hu and X. N. Li, *J. Catal.*, 2019, **373**, 240–249.
45 B. Nkosi, N. J. Coville and G. J. Hutchings, *Appl. Catal.*, 1988, **43**, 33–39.
46 L. Wang, F. Wang and J. Wang, *Catal. Commun.*, 2015, **65**, 41–45.
47 P. Li, M. Ding, L. He, K. Tie, H. Ma, X. Pan and X. Bao, *Sci. China: Chem.*, 2018, **61**, 444–448.
48 J. Zhao, Y. X. Yue, G. F. Sheng, B. L. Wang, H. X. Lai, S. X. Di, Y. Y. Zhai, L. L. Guo and X. N. Li, *Chem. Eng. J.*, 2019, **360**, 38–46.
49 K. Gesi, *Ferroelectrics*, 2001, **262**, 143–148.
50 G. Denuault, C. Milhano and D. Pletcher, *Phys. Chem. Chem. Phys.*, 2005, **7**, 3545–3551.
51 J. Hu, Q. Yang, L. Yang, Z. Zhang, B. Su, Z. Bao, Q. Ren, H. Xing and S. Dai, *ACS Catal.*, 2015, **5**, 6724–6731.
52 L. L. Yang, Q. W. Yang, J. Y. Hu, Z. B. Bao, B. G. Su, Z. G. Zhang, Q. L. Ren and H. B. Xing, *AIChE J.*, 2018, **64**, 2536–2544.
53 J. Zhao, X. L. Xu, X. N. Li and J. G. Wang, *Catal. Commun.*, 2014, **43**, 102–106.
54 Y. Hu, X. Yang, S. Cao, J. Zhou, Y. Wu, J. Han, Z. G. Yan and M. Zheng, *Appl. Surf. Sci.*, 2017, **400**, 148–153.
55 K. Zhou, W. Wang, Z. Zhao, G. H. Luo, J. T. Miller, M. S. Wong and F. Wei, *ACS Catal.*, 2014, **4**, 3112–3116.
56 M. Conte, C. J. Davies, D. J. Morgan, T. E. Davies, A. F. Carley, P. Johnston and G. J. Hutchings, *Catal. Sci. Technol.*, 2013, **3**, 128–134.